Ionization potential depression and Pauli blocking in degenerate plasmas at extreme densities

Gerd Röpke,[1,2] David Blaschke,[2,3,4] Tilo Döppner,[5] Chengliang Lin,[1] Wolf-Dietrich Kraeft,[1]
Ronald Redmer,[1] and Heidi Reinholz[1,6]

[1]*Institut für Physik, Universität Rostock, D-18051 Rostock, Germany*
[2]*Department of Theoretical Nuclear Physics, National Research Nuclear University (MEPhI), 115409 Moscow, Russia*
[3]*Institute of Theoretical Physics, University of Wroclaw, 50-204 Wroclaw, Poland*
[4]*Joint Institute for Nuclear Research, 141980 Dubna, Russia*
[5]*Lawrence Livermore National Laboratory, Livermore, California 94550, USA*
[6]*School of Physics, University of Western Australia, WA 6009 Crawley, Australia*

(Received 30 November 2018; published 4 March 2019)

New facilities explore warm dense matter (WDM) at conditions with extreme densities (exceeding ten times condensed matter densities) so that electrons are degenerate even at temperatures of 10–100 eV. Whereas in the nondegenerate region correlation effects such as Debye screening are relevant for the ionization potential depression (IPD), new effects have to be considered in degenerate plasmas. In addition to the Fock shift of the self-energies, the bound-state Pauli blocking becomes important with increasing density. Standard approaches to IPD such as Stewart-Pyatt and widely used opacity tables (e.g., OPAL) do not contain Pauli blocking effects for bound states. The consideration of degeneracy effects leads to a reduction of the ionization potential and to a higher degree of ionization. As an example, we present calculations for the ionization degree of carbon plasmas at $T = 100$ eV and extreme densities up to 40 g/cm^3, which are relevant to experiments that are currently scheduled at the National Ignition Facility.

DOI: 10.1103/PhysRevE.99.033201

I. INTRODUCTION

The availability of new experimental facilities allows exploration of matter under warm dense matter (WDM) conditions [1], where strong correlations in the ionic system and degeneracy of the electron system are of relevance. The region of densities and temperatures that can be probed has been extended toward multimegabar pressures and temperatures up to tens of eV at synchrotrons, with pulsed power, high-power optical, and free-electron lasers or other methods of high-pressure experimental technique. There, strong correlations and quantum effects have to be treated consistently, and simple models and approximations are pushed beyond their applicability limits.

Within the model of the partially ionized plasma, WDM consists of free electrons (particle density n_e) and ions a_i with different ionization states Z_i and densities n_i (including the neutral atom with $Z_0 = 0$). It is characterized by the ionization degree $\bar{Z} = n_e/n_a$, $n_a = \sum_i n_i$ being the particle density of all nuclei. However, concepts such as the partially ionized plasma and the ionization degree have to be analyzed and applied with care, because medium effects that influence the properties of isolated atoms and ions become more dominant with increasing density, leading to shift and broadening of energy levels and eventually to the disappearance of bound states (Mott effect, see Ref. [2]). Nevertheless, the concept of the composition of a partially ionized plasma is a useful tool to investigate the consequences of the appearance of bound states on thermodynamic properties, conductivity, optical spectra, Thomson scattering spectra, and other physical properties. However, near the Mott transition where the bound states merge with the continuum and are dissolved, the subdivision into (weakly) bound states and free states, including resonances, becomes questionable, and there exists no clear criterion to subdivide the electron subsystem into "free" and "bound" electrons. As discussed below, a many-body theory provides a consistent approach to WDM allowing for a systematic treatment of correlations including bound-state formation.

The properties of atoms and ions immersed in a dense plasma are modified owing to medium effects. This refers also to the ionization energy I_i of the ion a_i in the charge state Z_i, which at least is necessary to remove one electron from the ground state to the continuum of free electrons. As a consequence, the ionization potential I_i is modified compared to its vacuum value $I_i^{(0)}$. The ionization potential depression (IPD) $\Delta I_i = I_i^{(0)} - I_i$ is a particular property of WDM presently under intense discussion. In the low-density, weakly coupled limit, the shift of the energy of charged particles is given by screening. For an ion (atom) with charge state Z_i, the well-known Debye result for the energy shifts (see, e.g., Refs. [3,4]) leads to a reduction of the ionization potential $I_i^{\rm Debye} = I_i^{(0)} - \Delta I_i^{\rm Debye}$ as compared to the unperturbed ionization energy $I_i^{(0)}$. For the global ionization process $a_i \rightleftharpoons a_{i+1} + e$ (further particles must participate to realize conservation laws), we find the IPD in Debye approximation

$$\Delta I_i^{\rm Debye} = \kappa_{\rm class}(Z_i + 1)\frac{e^2}{4\pi\epsilon_0},$$
$$\kappa_{\rm class}^2 = \frac{e^2}{\epsilon_0 k_B T}\left(\sum_i Z_i^2 n_i + n_e\right). \quad (1)$$

A more general expression for the screening parameter (inverse Debye radius) $\kappa = 1/r_D$ which takes into account also the degeneracy of electrons, is given below in Sec. II C.

At high densities where the ions are strongly correlated, the ion sphere model, see Ref. [5], is more appropriate. In contrast to the Debye approximation, the density dependence of the shift is weaker ($\propto n^{1/3}$). Semiempirical interpolations have been proposed by Ecker and Kröll (EK) [6] and Stewart and Pyatt (SP) [7] which are frequently used for estimating the IPD. In the SP approach, the IPD is given according to

$$\Delta I_i^{\rm SP} = \frac{3}{2}\frac{(Z_i+1)e^2}{4\pi\epsilon_0 r_{\rm IS}}[(1+s^3)^{2/3} - s^2], \tag{2}$$

with the ion sphere radius $r_{\rm IS} = [3Z_i/(4\pi n_e)]^{1/3}$ and $s = (\kappa r_{\rm IS})^{-1}$. New experiments on high-density plasmas [8–14] cannot be explained using any of these simple approximations, and the need for a better approach is obvious when going to extreme conditions where the ions are strongly coupled.

According to Crowley [15], the chemical picture has to be replaced by a physical picture based on quantum statistical many-body theory [3,4]. In this work, such a systematic treatment of different plasma effects is worked out using Green-function techniques. Alternatively, numerical simulations such as path integral Monte Carlo (PIMC) simulations [16,17] have been used to give a systematic approach to properties of WDM. Because of the fermion sign problem, PIMC simulations of two-component plasmas are restricted presently to high temperatures and high densities.

The electron-ion interaction is strong in the low-temperature region where bound-state formation is relevant. A very successful and practicable approximation is density-functional theory (DFT) for electronic structure calculations in combination with molecular dynamics simulations for the ions (DFT-MD). It has proven to predict results for WDM states; see, e.g., Ref. [18]. Using standard expressions for the exchange-correlation part of the (free) energy, detailed properties of the electron system like the density of states as well as the ionic structure factor are obtained. Electron-electron correlations are treated approximately using appropriate expressions for the energy-density functional. For the treatment of IPD using this formalism see Refs. [9–12].

Coming back to the quantum statistical approach using Green-function techniques, the shift of the continuum is related to the single-particle self-energy. A systematic discussion of the energy spectrum of hydrogen atoms in dense plasmas within the Green function approach has been given by Seidel *et al.* [19]. An improved treatment of the self-energy using the Montroll-Ward expression, which gives the Debye shift in the low-density limit, has been proposed recently by Lin *et al.* [20]. Using the fluctuation-dissipation theorem, the inverse dielectric function is related to the dynamical structure factor. With known expressions for the ion-ion structure factor (SF), the calculated IPD show a better agreement with experimental data.

If going to even higher densities, in addition to the strong coupling of the ions, then the degeneracy of electrons becomes important. Related effects, in particular Pauli blocking and Fock shifts, are not included in the approaches to the IPD [7,20] discussed so far. The electron degeneracy parameter is defined as

$$\Theta = \frac{T}{T_{\rm Fermi}} = \frac{2m_e k_B T}{\hbar^2}(3\pi^2 n_e)^{-2/3}. \tag{3}$$

In the region of the temperature-density plane, where $\Theta \leqslant 1$, a classical description is no longer valid. Instead, quantum effects, in particular the Pauli principle as a consequence of the antisymmetry of the many-electron (fermonic) wave function, lead to so-called exchange terms. The related condition $n_e\Lambda_e^3 \geqslant 1$ with $n_e\Lambda_e^3 = n_e(2\pi\hbar^2/m_e k_B T)^{3/2} = 8/(3\pi^{1/2})\Theta^{-3/2}$ is well known as a condition where the classical gas approach is not applicable, and the quantum description based on the Fermi distribution function must be applied. For instance, in carbon plasmas at $T = 100$ eV, the electrons become degenerate at electron density $n_e \approx 4\times 10^{24}$ cm^{-3} corresponding to a carbon mass density of 20 g cm^{-3}. New experiments are planned and will be performed, for instance, at the National Ignition Facility (NIF) in Livermore to explore WDM [21] at very high densities where plasmas become degenerate even at temperatures of the order of 100 eV.

New physics becomes of importance in degenerate systems. Whereas at lower densities, in the classical region, dynamical screening is the most important medium effect, at extreme high densities exchange effects become of increasing relevance. Note that SP is widely used to calculate IPD and ionization at these extreme conditions, see also Ref. [22]. However, degeneracy effects such as bound-state Pauli blocking and Fock shifts are not consistently included. Pauli blocking effects have been extensively investigated for light clusters (^{2}H, ^{3}H, ^{3}He, ^{4}He) in nuclear matter [23], see also Ref. [24], as a mechanism of hadron dissociation. For hydrogen plasmas they have been discussed in Ref. [25].

In this work we give a systematic treatment of the effects of degeneracy within a Green function approach and its consequences for IPD in the region of very high densities where standard approaches such as SP or widely used opacity tables like OPAL [22] become inapplicable. In Sec. II we consider the effective wave equation for few-particle (bound) states in a plasma environment and discuss Pauli blocking and Fock shifts. We apply these results to carbon plasmas at high densities in Sec. III, where a significant increase of the ionization degree compared to the frequently used SP model is obtained. Pauli blocking effects are also of relevance for K-edge shifting [26] to be discussed in Sec. IV.

II. IN-MEDIUM SCHRÖDINGER EQUATION

A. Low-density limit of the plasma composition

We consider an element a (e.g., carbon C in Sec. III) in the WDM region. Let us first recall the low-density limit where the in-medium effects can be neglected. The model of partially ionized plasma (PIP) considers a plasma which is composed of different ions (a_i) with charge number Z_i at partial density n_i (including neutral atoms), as well as free electrons at density n_e. The components of the PIP can react, changing the state of excitation, including ionization and recombination processes. Thermodynamic equilibrium is described by relations between the corresponding chemical potentials of the different components.

The ideal electron chemical potential for arbitrary degeneracy follows from the expression for the density,

$$n_e = g_e \int \frac{d^3p}{(2\pi)^3} \frac{1}{\exp[\beta\hbar^2 p^2/(2m_e) - \beta\mu_e] + 1}, \quad (4)$$

where $\beta = 1/(k_B T)$. The factor $g_e = 2$ accounts for spin degeneracy. The Fermi distribution can be replaced by the Boltzmann distribution in the classical case $\exp(\beta\mu_e) \ll 1$ so that $\exp(\beta\mu_e) \approx n_e(2\pi\beta\hbar^2/m_e)^{3/2}/2$.

The density $n_{i,\hat{n}}$ of ions with its fully known quantum state $\hat{n}$, characterized by the complete set of quantum numbers including total momentum, spin, angular momentum, etc., is given by the chemical potential $\mu_{i,\hat{n}}$. For instance, for the two-body problem, the complete set of quantum numbers $\hat{n} = \{\mathbf{P}, \gamma, \nu\}$ contains in addition to the center-of mass momentum $\mathbf{P}$ and the channel quantum number γ further intrinsic quantum numbers ν which describe the intrinsic excitation. The channel quantum number γ contains, e.g., spin and angular momentum depending on the observables which are conserved in the two-body interaction.

In the low-density limit, where the interaction between the particles and clusters can be neglected (with exception of reacting collisions), the summation over the total momentum $\mathbf{P}$ can be performed, and we obtain in thermodynamic equilibrium the well-known relation for the ideal gas,

$$n_{i,\gamma,\nu} = \int \frac{d^3P}{(2\pi)^3} e^{-\beta\hbar^2 P^2/(2M) + \beta\mu_{i,\gamma,\nu}} = \frac{1}{\Lambda^3} e^{\beta\mu_{i,\gamma,\nu}}, \quad (5)$$

where $\Lambda = [2\pi\beta\hbar^2/M]^{1/2}$ is the thermal wavelength of the ions. We restrict to the region of thermodynamic parameters where the ions can be treated classically; M is the ion mass (dependence on charge number is neglected). The specific chemical potentials $\mu_{i,\gamma,\nu}$ are gauged so that only the kinetic energy of the cluster owing to the center-of-mass motion is considered. The potential energy, in particular the binding energies of ions, must be considered separately.

The description is simplified if we consider also the sum over intrinsic degrees of freedom, similar to the spin degeneracy in the case of the electron component. With respect to the ground state $\{\gamma, \nu\} = (0)$ of the ion a_i with the chemical potential μ_i for this ground state, the excitation energy is denoted by $E_{i,\gamma,\nu}$ (we assume that the energy of the intrinsic motion does not depend on $\mathbf{P}$). Chemical equilibrium is achieved if the condition $\mu_{i,\gamma,\nu} = \mu_i + E_{i,\gamma,\nu}$ holds. For the total contribution of ions a_i with charge $Z_i e$ we have

$$n_i = \sum_{\gamma,\nu} n_{i,\gamma,\nu} = \frac{1}{\Lambda^3} \sum_{\gamma,\nu} e^{\beta(\mu_i + E_{i,\gamma,\nu})} = \frac{1}{\Lambda^3} \sum_{\gamma} \sigma_{i,\gamma}(T) e^{\beta\mu_i}, \quad (6)$$

with the intrinsic partition function in the channel γ,

$$\sigma_{i,\gamma}(T) = \sum_{\nu} e^{\beta E_{i,\gamma,\nu}}. \quad (7)$$

In a further step, we can also perform the sum over the different channels to obtain the full intrinsic partition function $\sigma_i(T) = \sum_\gamma \sigma_{i,\gamma}(T)$ of the ion a_i so that

$$n_i = \frac{1}{\Lambda^3} \sigma_i(T) e^{\beta\mu_i}. \quad (8)$$

Compared to the expression for the free electrons Eq. (4), the spin summation is contained in the summation over γ, and the intrinsic excitations are taken into account because the ion a_i is in general a composite particle. An important issue is that the summation over ν in Eq. (6) has to be performed not only over the bound states but also over the continuum of scattering states.

For the summation over the continuum of scattering states, the quantum number ν is replaced by the energy E of relative motion. We denote the scattering phase shift in the channel γ as $\delta_{i,\gamma}(E)$. According to Beth and Uhlenbeck [27], for the intrinsic partition function $\sigma_{i,\gamma}(T)$ the following expression is derived

$$\sigma_{i,\gamma}(T) = \sum_{\nu}^{\text{bound}} (e^{-\beta E_{i,\gamma,\nu}} - 1) + \frac{1}{\pi k_B T} \int_0^\infty dE\, e^{-\beta E} \delta_{i,\gamma}(E). \quad (9)$$

In particular, calculating the pressure as function of density and temperature by integration of $n(T, \mu_i, \mu_e)$, the result Eq. (9) gives an exact expressions for the second virial coefficient [27]. More details concerning the intrinsic partition function in the low-density limit are presented in the Appendix.

Within a quantum statistical approach, a generalized Beth-Uhlenbeck formula is derived which can be used also at higher densities. It has a similar form like Eq. (9) but contains medium-dependent quasiparticle energies $E_{i,\gamma,\nu}$ and scattering phase shifts $\delta_{i,\gamma}(E)$, see Eq. (15) in Sec. II B. In this work, we use this generalized Beth-Uhlenbeck formula to calculate the composition and the ionization degree in WDM.

At this point, an important comment is necessary. Different expressions are known for the intrinsic partition function $\sigma_i(T)$; see the Appendix. They all give exact results for the second virial coefficient, but the separation of a bound-state part is difficult. Usually, only the bound-state contribution to the intrinsic partition function $\sigma_i(T)$ is taken into account to define the degree of ionization which, as a consequence, is model dependent. In this work we propose another concept shown in Sec. II B. The total density can be decomposed into a free quasiparticle density and a correlated one. This can be used to define the ionization degree, including the contribution of scattering states. In particular, the correlation part contains, in addition to contributions of the bound states, also a contribution owing to resonances if they exist. No clear physical criterion is known to define bound states near the continuum edge, because there is no principal difference between the physical properties of a broadened, weakly bound state and a resonance state in the continuum.

Measured properties, e.g., the second virial coefficient and the corresponding thermodynamic variables such as pressure and free energy, are not model-dependent. The calculation of these properties should take into account both, bound as well as scattering states. They are independent of the artificial subdivision into bound and scattering state contributions. A cluster decomposition can be used to determine the single quasiparticle contribution and few-particle correlations in a model-independent way. This concept gives the possibility to generalize the concept of the composition of partially ionized plasmas (PIP) valid in the low-density limit to a region of higher densities.

Reactions in PIP include also ionization and recombination processes $a_{i,\gamma,\nu} + s \rightleftharpoons a_{i+1,\gamma',\nu'} + e + s'$. The conservation laws (in particular of energy and momentum) demand, for instance, the collision with a third particle s (spectator) or the emission and absorption of a photon. In thermodynamical equilibrium, these processes lead to a relation between the chemical potentials μ_i introduced above for the ground state of the corresponding ionic components of the PIP. Using the notation I_i (ionization potential) for the lowest excitation energy $E_{i,0}$ of the ionic ground state to become ionized, the condition for chemical equilibrium reads

$$\mu_i = \mu_{i+1} + \mu_e + I_i. \tag{10}$$

The bound-state energy $-I_i$ (ground-state energy of the ion a_i relative to the continuum of $a_{i+1} + e$) can be implemented as potential energy in the scaling of the chemical potentials of each ion charge state. Inserting relation Eq. (10) into Eq. (8), the Saha equation is obtained which determines the concentration of the different components of the PIP.

If there are several ionization states Z_i, then the repeated use of Eq. (10) leads to a coupled system of Saha equations. Finally, only the chemical potentials of the electrons and the ionic nuclei remain, corresponding to the conserved total number of electrons and nuclei of the WDM. Taking into account electrical neutrality, the thermodynamic state of WDM is defined by the total mass density $n_a^{\rm total}$ and the temperature T. The composition of the PIP model, including the degree of ionization $\bar{Z}$, follows from the solution of the coupled system of Saha Eqs. (8) and (10). Results for the composition within the PIP model in the low density region, neglecting the interaction between the components, are well known. According to the mass-action law, the ionization degree $\bar{Z}$ increases with increasing T, but decreases with increasing $n_a^{\rm total}$. Results for the ionization degree of the ideal carbon plasma are given below in Fig. 2.

B. Quantum statistical approach for interacting plasmas

The definition of the composition of a dense system is not free of model assumptions so that one should use a systematic quantum statistical approach to calculate physical properties. Nevertheless, the composition of a PIP and a corresponding ionization degree are useful concepts for low-density plasmas, but have to be handled with care in the high-density region. In the present work, we consider thermodynamics to define the composition and the ionization degree of the PIP. Instead of the contribution of free electrons to the total density, free quasiparticles with medium-dependent energies are considered. The remaining part of composition describes correlations, in particular the contribution of bound states. A quantum statistical approach to the composition of a PIP is obtained from the equation of state which relates the total densities of electrons $n_e^{\rm total}$ and nuclei $n_a^{\rm total}$ to the temperature $T = 1/(k_B\beta)$ and the chemical potentials μ_e, μ_a,

$$n_e^{\rm total}(T,\mu_e,\mu_a) = \frac{1}{\Omega}\sum_1 \int_\infty^\infty \frac{d\omega}{2\pi}\frac{1}{e^{\beta(\omega-\mu_e)}+1} A_e(1,\omega), \tag{11}$$

with the spectral function $A_e(1,\omega)$, the single-particle states are denoted by wave number vector, and spin, $|1\rangle = |\mathbf{p}_1,\sigma_1\rangle$, and Ω the system volume. A corresponding relation holds also for $n_a^{\rm total}$. Both the variables μ_e, μ_a are related to each other because of charge neutrality. With the charge number Z_a of the nuclei, we have $n_e^{\rm total} = Z_a\, n_a^{\rm total}$. The relation Eq. (11) gives an immediate access to the mass action law or, in plasma physics, the Saha equation. Having the equations of state $\mu_c(T, Z_a\, n_a^{\rm total}, n_a^{\rm total})$, $c = a, e$, at our disposal, thermodynamic potentials such as the free energy $F(T, Z_a\, n_a^{\rm total}, n_a^{\rm total})$ are obtained by integration. From this, all other thermodynamic properties are derived. Note that also the density of states is obtained from the spectral function.

The spectral function, which fulfills the normalization condition $\int \frac{d\omega}{2\pi} A_e(1,\omega) = 1$, is related to the self-energy $\Sigma_e(1,z)$,

$$A_e(1,\omega) = \frac{2\,\mathrm{Im}\,\Sigma_e(1,\omega+i0)}{[\omega - E_e(1) - \mathrm{Re}\,\Sigma_e(1,\omega)]^2 + [\mathrm{Im}\,\Sigma_e(1,\omega+i0)]^2}. \tag{12}$$

The self-energy, which is defined by the Dyson equation for the Green function as $G_e(1,iz_\nu) = 1/[iz_\nu - E_e(1) - \Sigma_e(1,iz_\nu)]$, can be calculated for given interaction using the technique of Feynman's diagrams. For small $\mathrm{Im}\,\Sigma_e(1,\omega+i0)$, i.e., small damping of the quasiparticles, we have [28]

$$A_e(1,\omega) \approx \frac{2\pi\,\delta\big[\omega - E_e^{\rm quasi}(1)\big]}{1 - \frac{d}{dz}\mathrm{Re}\,\Sigma_e(1,z)|_{z=E_e^{\rm quasi}-\mu_e}} - 2\mathrm{Im}\,\Sigma_e(1,\omega+i0)\frac{d}{d\omega}\frac{\mathcal{P}}{\omega+\mu_e-E_e^{\rm quasi}(1)}, \tag{13}$$

with the quasiparticle energy

$$E_e^{\rm quasi}(1) = E_e(1) + \mathrm{Re}\,\Sigma_e(1,\omega)|_{\omega=E_e^{\rm quasi}} = E_e(1) + \Delta_e(1) \tag{14}$$

and $\mathcal{P}$ denoting the principal value. For the self-energy $\Sigma_e(1,z)$, a cluster decomposition can be performed, which leads to mass action laws [29].

Considering two-particle contributions (T-matrix) to the self-energy, we obtain the generalized Beth-Uhlenbeck formula for the virial expansion in the quasiparticle picture [28,30]

$$n_e^{\rm total}(T,\mu_e,\mu_a) = \frac{1}{\Omega}\sum_1 f_e[E^{\rm quasi}(1)] + \frac{1}{\Lambda^3}\sum_{i,\gamma} Z_i e^{\beta\mu_i} \times\left[\sum_\nu^{\rm bound}(e^{-\beta E_{i,\gamma,\nu}}-1) + \frac{\beta}{\pi}\int_0^\infty dE\, e^{-\beta E} \times\left\{\delta_{i,\gamma}(E) - \frac{1}{2}\sin[2\delta_{i,\gamma}(E)]\right\}\right], \tag{15}$$

$f_e(E) = \{\exp[\beta(E-\mu_e)]+1\}^{-1}$, and $E_{i,\gamma,\nu}$ is the excitation energy of the ion a_i, channel γ. The contribution of free electrons is replaced by the contribution of quasi-single particles with shifted energies Eq. (14). The contribution of the scattering states is reduced (sin-term in the last expression)

because part of the interaction in the continuum, in particular the contribution of Born approximation, is already accounted for introducing the quasisingle particle contribution [30,31]. As discussed in the following Sec. II C, the bound-state energies $E_{i,\gamma,\nu}$ and scattering phase shifts $\delta_{i,\gamma}(E)$ are modified by the interaction with the surrounding plasma as well and are calculated from an in-medium Schrödinger equation.

At this point we can perform a subdivision of the total electron density into a free part given by the (damped) quasisingle particle contribution, and the remaining correlated density contribution. This definition of a free-electron density n_e and the corresponding ionization degree is possible as long as the single-electron spectral function Eqs. (12) and (13) show a peak structure owing to the quasiparticle excitation. Within a cluster decomposition of the self-energy, a similar decomposition can also be performed for the higher order T-matrix contributions; see the cluster-virial expansion discussed for nuclear matter in Ref. [31].

As a consequence, the cluster contributions n_i of the ionization state Z_i to the ion density and the density of electrons is not restricted to only the bound-state contribution but contains also continuum contributions given in terms of the scattering phase shifts as shown in the second part of the right-hand side of Eq. (15).

C. In-medium Schrödinger equation and density effects

The ideal plasma with the unperturbed energies $E_{i,\gamma,\nu}$ of the bound states and the kinetic energies of the free states cannot describe plasmas at high densities where interaction effects are important. For simplicity we consider here the ionization degree of carbon at very high densities and/or temperatures where the carbon atoms are either fully ionized or in the C^{5+} state, i.e., with one bound electron.

We consider the in-medium two-particle problem of the formation of the C^{5+} state, described by the two-particle in-medium Schrödinger equation. A Green function approach [3,4] leads to the following two-particle equation (quantum number $\hat{n} = \{\mathbf{P}, \gamma, \nu\}$, total momentum $\mathbf{P}$, spin variables not given explicitly)

$$[E_e(p) + \Sigma_e(p,z) + E_{C^{6+}}(k) + \Sigma_{C^{6+}}(k,z)]\psi^{5+}_{\hat{n}}(\mathbf{p},\mathbf{k}) + [1 - f_e(p) \mp f_{C^{6+}}(k)] \sum_{\mathbf{q}} V^{\rm eff}_{C^{6+},e}(\mathbf{p},\mathbf{k},\mathbf{q},z)\psi^{5+}_{\hat{n}}(\mathbf{p}+\mathbf{q},\mathbf{k}-\mathbf{q})$$
$$= E^{5+}_{\hat{n}}\psi^{5+}_{\hat{n}}(\mathbf{p},\mathbf{k}), \tag{16}$$

with the effective interaction

$$V^{\rm eff}_{C^{6+},e}(1,2,\mathbf{q},z) = V_{C^{6+},e}(q)\Bigg\{1 - \int_{-\infty}^{\infty}\frac{d\omega}{\pi}{\rm Im}\,\varepsilon^{-1}(q,\omega+i0)[n_B(\omega)+1]\Bigg[\frac{1}{z-\omega-E_{C^{6+}}(1)-E_e(2-\mathbf{q})}$$
$$+\frac{1}{z-\omega-E_{C^{6+}}(1+\mathbf{q})-E_e(2)}\Bigg]\Bigg\}. \tag{17}$$

We neglected higher-order terms $\propto f_c(p) = \{\exp[\beta(E_c(p) - \mu_c)] \pm 1\}^{-1}$, the Fermi/Bose function for $c = e, C^{6+}$. $V_{C^{6+},e}(q) = -Z_6 e^2/\epsilon_0 q^2$ is the Coulomb interaction. Without any chemical potential, $n_B(\omega) = [\exp(\beta\omega) - 1]^{-1}$ is the Bose distribution function.

The in-medium Schrödinger Eq. (16) contains the contribution of self-energies Σ_c as well as the contribution of effective interaction including Pauli blocking. As a consequence, the energy eigenvalues $E^{5+}_{\hat{n}}$ of bound states as well as of continuum states are dependent on density and temperature of the surrounding plasma. These "dressed" states are denoted as quasiparticle excitations. The Mott effect is the disappearance of a bound state if the ionization potential $I^{5+}_{\gamma,\nu} = E^{5+}_{\rm cont} - E^{5+}_{\gamma,\nu}$ goes to zero (Mott density). The continuum edge $E^{5+}_{\rm cont} = \Delta_{C^{6+}}(k=0) + \Delta_e(p=0)$ is given by the quasiparticle shifts Eq. (14). The bound-state energy $E^{5+}_{\gamma,\nu}$ is a function of temperature and density. The bound-state part of the intrinsic partition function Eqs. (6), (9), and (15) has the form

$$\sigma^{\rm bound}_{C^{5+}}(T) = \sum_{\gamma,\nu}^{\rm bound}\left[e^{\beta I^{5+}_{\gamma,\nu}} - 1\right]\theta\left(I^{5+}_{\gamma,\nu}\right),$$
$$\theta(x) = \begin{Bmatrix} 1 & \text{if } x > 0, \\ 0 & \text{else,} \end{Bmatrix} \tag{18}$$

with the channel γ (spin, angular momentum) and the intrinsic excitation ν. Later on we use this approximation for the generalized Beth-Uhlenbeck (BU) Eq. (15) to define the density contribution of bound states. As a function of temperature and density, the intrinsic partition function Eq. (18) is continuous at the Mott density. A more detailed approach based on in-medium scattering phase shifts, see last term in Eq. (15), can also take into account resonances in the continuum. In this work we neglect the contribution of in-medium scattering phase shifts. In the case of a separable potential, the phase shifts are available, see Ref. [32], so that the contribution to the intrinsic partition function can be evaluated. This issue may be subject of future investigations.

In the zero density limit where in-medium effects are absent, Eq. (16) reproduces the Schrödinger equation for the hydrogenlike atom. Density effects arising from the dynamical self-energy $\Sigma_c(p,z)$, the Pauli blocking $(1 - f_e \mp f_{C^{6+}})$, and the dynamical screening expressed by the dielectric function $\varepsilon(q,z)$ in Eq. (17) have to be treated in appropriate approximations. As mentioned above, the carbon ions can be treated classically so that the contribution $\mp f_{C^{6+}}(k)$ can be dropped. The Pauli blocking becomes relevant if the free electrons are degenerate. The contribution to the shift of bound-state energies is discussed in Sec. II D.

Using the technique of Feynman diagrams, systematic approaches for the dielectric function $\varepsilon(q,z)$ can be found [3].

A standard expression for the dielectric function is the random phase approximation (RPA) where the polarization function is calculated in lowest order with respect to the interaction. In the static limit, the effective interaction Eq. (17) gives the Debye result $V^{\rm Debye}_{{\rm C}^{6+},e}(1,2,\mathbf{q},z) = V_{{\rm C}^{6+},e}(q)/(1+\kappa^2/q^2)$ with the Debye screening parameter $\kappa^2 = \sum_i Z_i^2 e^2 n_i/(\epsilon_0 k_B T) + \kappa_e^2$,

$$\kappa_e^2 = \frac{4\pi}{k_B T} 2\left(\frac{2\pi\hbar^2}{m_e k_B T}\right)^{-3/2} \frac{e^2}{4\pi\epsilon_0}\frac{1}{\sqrt{\pi}}\int_0^\infty dt\,\frac{t^{-1/2}}{e^{t-\beta\mu_e}+1}$$
$$= 12\pi^{5/2}\frac{e^2}{4\pi\epsilon_0} n_e\beta\frac{F_{-1/2}(\beta\mu_e)}{(\beta E_F)^{3/2}}. \tag{19}$$

The expression for the Debye screening parameter κ includes the contribution of free electrons (κ_e) which eventually become degenerate. Then, in contrast to the classical limit Eq. (1), the electron contribution is given by a Fermi integral which, in the strongly degenerate limit, yields the Thomas-Fermi screening length instead of the Debye screening length; see Refs. [3,4,22]. The electron chemical potential μ_e is given by Eq. (4).

For the dynamical self-energies $\Sigma_e(p,z)$, $\Sigma_{{\rm C}^{6+}}(k,z)$ occurring in Eq. (16), a systematic expansion is possible in terms of Feynman diagrams [3]. For the electron quasiparticle shift $\Delta_e(p)$ Eq. (14) the expansion $\Delta_e(p) = \Delta_e^{\rm Fock}(p) + \Delta_e^{\rm corr}(p)$ results. As lowest order with respect to interaction, the Fock shift for the electrons

$$\Delta_e^{\rm Fock}(p) = -\sum_q \frac{e^2}{\epsilon_0 q^2} f_e(\mathbf{p}+\mathbf{q}) \tag{20}$$

is obtained (the Hartree term vanishes because of charge neutrality of the plasma). This shift is a typical quantum effect. Because the ions are treated classically under the conditions considered here, the corresponding contribution disappears. The further treatment of the electron contribution Eq. (20) is postponed to the following Sec. II D.

We consider in this section the next order of the expansion of $\Delta_e(p)$, the correlation shift (Montroll-Ward shift) $\Delta_e^{\rm corr}(p)$. It describes the formation of a screening cloud and has been intensely investigated. In the so-called GW approximation, the RPA expression for the screened interaction can be used, and we find the Debye shift

$$\Delta_e^{\rm corr}(p) = -\frac{\kappa e^2}{8\pi\epsilon_0} \tag{21}$$

in the low-density, nondegenerate limit. Because this is a classical effect, describing the formation of the screening cloud as solution of the Poisson-Boltzmann equation, it applies also to the ions a_i, which are shifted according to the charge number Z_i,

$$\Delta_i^{\rm corr}(p) = -\frac{\kappa Z_i^2 e^2}{8\pi\epsilon_0}, \tag{22}$$

in particular, $Z_6 = 6$ for C^{6+}. With these expressions, the IPD in Debye approximation Eq. (1) is found for the ionization and recombination reaction $a_i + s \rightleftharpoons a_{i+1} + e + s'$ discussed above.

It is an advantage of the many-particle approach that systematic improvements can be given. The correlation shift has the general form

$$\mathrm{Re}\,\Sigma_c^{\rm corr}(p,\omega) = -\mathcal{P}\int\frac{d^3\mathbf{q}}{(2\pi)^3}\int\frac{d\omega'}{\pi}V_{cc}(q)$$
$$\times\,\mathrm{Im}\,\varepsilon^{-1}(q,\omega'+i0)\frac{1+n_{\rm B}(\omega')}{\omega-\omega'-E_c(\mathbf{p}+\mathbf{q})/\hbar}. \tag{23}$$

$\mathcal{P}$ denotes the principal value, the index c denotes electron as well as, for our system here, the different carbon ions. Instead of approximating the dielectric function by the RPA expression, which gives the Debye result, we can use the fluctuation-dissipation theorem which relates the inverse dielectric function to the dynamical SF [20]. For a two-component plasma (free electrons with charge $-e$, ions with effective charge $\bar{Z}e$ and charge neutrality $\bar{Z}n_i = n_e$), the imaginary part of the inverse dielectric function can be expressed via the dynamical SFs, see also Ref. [33],

$$\mathrm{Im}\,\varepsilon^{-1}(\mathbf{q},\omega+i0) = \frac{e^2}{\varepsilon_0 q^2}\frac{\pi}{\hbar\,[1+n_{\rm B}(\omega)]}[\bar{Z}^2 n_i S_{\rm ii}(\mathbf{q},\omega)$$
$$-2\bar{Z}\sqrt{n_e n_i}S_{\rm ei}(\mathbf{q},\omega) + n_e S_{\rm ee}(\mathbf{q},\omega)]. \tag{24}$$

After using a plasmon-pole approximation for $S(\mathbf{q},\omega)$ [20,34], the dynamical response of the system is determined by the plasmon pole frequency $\omega_{\rm pl} = (\sum_c e^2 Z_c^2 n_c/\epsilon_0 m_c)^{1/2}$. Then, the integral over the frequency in Eq. (23) is executed. Accounting for nonlinear screening [20], the ionic contribution to the single-particle shift is related to the static SF

$$\Delta_i^{\rm SF,ion-ion} = \frac{3(Z_i+1)e^2\Gamma_i}{2\pi^2\epsilon_0 r_{\rm WS}\sqrt{(9\pi/4)^{2/3}+3\Gamma_i}}\int_0^\infty\frac{dq}{q^2}S_{\rm ii}^{ZZ}(q), \tag{25}$$

with $r_{\rm WS} = (4\pi n_i)^{-1/3}$ and $\Gamma_i = Z_i^2 e^2/(4\pi\epsilon_0 k_B T r_{\rm WS})$. We can use known expressions for the SF such as the approximation given in Ref. [35] for recent calculations [20]. As explained there, an improved description of experiments [8–14] has been obtained. For future work [36], HNC calculations or DFT-MD simulations can be applied to implement the structure factor in Eq. (25).

Instead of the phenomenological SP Eq. (2), the IPD is related to the dynamical ion structure factor. Within the Green function approach, Eq. (25) can be improved in a systematic way considering higher order diagrams. In particular, the electronic contribution to the correlated part of the self-energy shift $\Delta_e^{\rm corr}(p)$ can be improved. Expressions for the Montroll-Ward term are found, e.g., in Ref. [3].

In this work, we are not concerned with the improvement of the correlated part of the self-energies that will be considered in a forthcoming work, see also Refs. [3,4,20,37,38], but focus on the effects of degeneracy. As discussed above, the Debye approximation for the correlation shift can be replaced by the Stewart-Pyatt expression or more advanced approximations based on the dynamical structure factor if going to high densities. We consider here the SP approximation Eq. (2) frequently used in IPD calculations, to have a result of reference. Results for the corresponding IPD are shown in Fig. 1 below, where also the comparison with SF calculations [20] is given.

D. Degeneracy effects

To investigate the effects of degeneracy, i.e., Pauli blocking and Fock shifts, we simplify the two-particle Eq. (16). The ions are considered as nondegenerate so that their contribution to the Pauli blocking term is dropped. In addition, we replace the dynamical screening by a statically screened (Debye) interaction $V^{\rm scr}_{{\rm C}^{6+},e}(\mathbf{q})$ and introduce the quasiparticle shifts Eq. (14):

$$[E_e(p)+\Delta_e(p)+E_{{\rm C}^{6+}}(k)+\Delta_{{\rm C}^{6+}}(k)]\psi^{5+}_{\hat{n}}(\mathbf{p},\mathbf{k})+[1-f_e(p)]\sum_{\mathbf{q}}V^{\rm scr}_{{\rm C}^{6+},e}(\mathbf{q})\psi^{5+}_{\hat{n}}(\mathbf{p}+\mathbf{q},\mathbf{k}-\mathbf{q})=E^{5+}_{\hat{n}}\psi^{5+}_{\hat{n}}(\mathbf{p},\mathbf{k}). \quad (26)$$

In adiabatic approximation, the motion of electrons is separated from the motion of ions. More systematically, we introduce Jacobian coordinates, the center-of mass momentum $\mathbf{P}$, and the relative momentum $\mathbf{p}_{\rm rel}$. We use a separation ansatz for the wave function $\psi^{5+}_{\hat{n}}(\mathbf{p},\mathbf{k})=\Phi_{\hat{n}}(\mathbf{P})\phi_{\hat{n}}(\mathbf{p}_{\rm rel})$. The center-of-mass motion is given by a plane wave. In limit $m_e \ll M$, where $\mathbf{p}_{\rm rel}\approx\mathbf{p}$, we obtain for the relative motion

$$[E_e(p)+\Delta_e(p)]\phi_{\hat{n}}(\mathbf{p})+[1-f_e(p)]\sum_{\mathbf{q}}V^{\rm scr}_{{\rm C}^{6+},e}(\mathbf{q})\phi_{\hat{n}}(\mathbf{p}+\mathbf{q}) = E^{5+}_{\hat{n},{\rm rel}}\phi_{\hat{n}}(\mathbf{p}), \quad (27)$$

so that $E^{5+}_{\hat{n}}=E_{{\rm C}^{6+}}(k)+\Delta_{{\rm C}^{6+}}(k)+E^{5+}_{\hat{n},{\rm rel}}$.

The Fock shift of an electron with momentum p is given by Eq. (20). In the limit of strong degeneracy, $T\ll T_{\rm F}$, we approximate the Fermi distribution function as step function, $f_e(p)=\theta(p_{\rm F}-p)$. The Fermi wave number follows as $p_{\rm F}=(3\pi^2 n_e)^{1/3}$. At zero temperature, we find for the Fock shift

$$\Delta^{\rm Fock}_{e,T=0}(p)=-\frac{e^2}{4\pi\epsilon_0}\frac{1}{\pi p}{\rm Re}\left[p\,p_{\rm F}+\left(p_{\rm F}^2-p^2\right)\arctan\left(\frac{p}{p_{\rm F}}\right)\right]. \quad (28)$$

The contribution of the Fock shift $\Delta^{\rm Fock}_e(0)$ to the shift of the continuum edge is given by the value at $p=0$. At $T=0$ we have for the shift of the continuum edge $\Delta^{\rm Fock}_{e,T=0}(0)=-\frac{2}{\pi}\frac{e^2}{4\pi\epsilon_0}p_F$. At finite T, the Fock shift of the continuum edge, Eq. (20) at $p=0$, is calculated numerically.

Considering the bound states of the in-medium Schrödinger Eq. (26), the ions a_5, two contributions arise owing to the electron degeneracy: the Fock shift Eq. (20) which modifies the kinetic energy in the Schrödinger equation as well as the Pauli blocking term in front of the interaction potential. Because the Fermi function occurring in both contributions depends on T and n_e, the solution E^{5+}_n of the Schrödinger Eq. (26) also depends on these parameters. Both contributions to the shift of E^{5+}_n, the Pauli blocking and the Fock shift, are found solving Eq. (27) for the relative motion.

As an example we give the shift $\Delta_0=\Delta_0^{\rm bound,\,Fock}+\Delta_0^{\rm bound,\,Pauli}$ of the ground-state energy E^{5+}_0 in perturbation theory. The two-particle Schrödinger equation without any medium corrections has the well-known hydrogenlike ground-state solution $E_0^{(Z-1)+}=-Z^2\frac{e^4}{(4\pi\epsilon_0)^2}\frac{m_e}{2\hbar^2}=-13.602\,Z^2$ eV with $Z=6$ for the case considered here, and

$$\phi_0(p)=8\sqrt{\pi a_Z^3}\frac{1}{\left(1+a_Z^2p^2\right)^2},\quad \psi_0(r)=\frac{1}{\sqrt{\pi a_Z^3}}e^{-r/a_Z}, \quad (29)$$

$a_Z=\frac{4\pi\epsilon_0}{Ze^2}\frac{\hbar^2}{m_e}=a_B/Z$.

The Fock shift $\Delta_0^{\rm bound,\,Fock}$ of the bound-state energy results in perturbation theory as average of the momentum-dependent Fock shift Eq. (20) with this unperturbed wave function Eq. (29),

$$\Delta_0^{\rm bound,\,Fock}=-\sum_{p,q}\phi_0^2(p)\frac{e^2}{\epsilon_0 q^2}f_e(\mathbf{p}+\mathbf{q}) =-\frac{32}{\pi}\int_0^\infty dp\frac{p^2a_Z^3}{\left(1+a_Z^2p^2\right)^4}\Delta^{\rm Fock}_e(p). \quad (30)$$

An explicit expression can be given for zero temperature ($T=0$),

$$\Delta^{\rm bound,\,Fock}_{0,T=0}=-\frac{e^2}{4\pi\epsilon_0}\frac{2}{\pi a_Z}\frac{5a_Z^3p_F^3+3a_Z^5p_F^5}{\left(a_Z^2p_F^2+1\right)^2}. \quad (31)$$

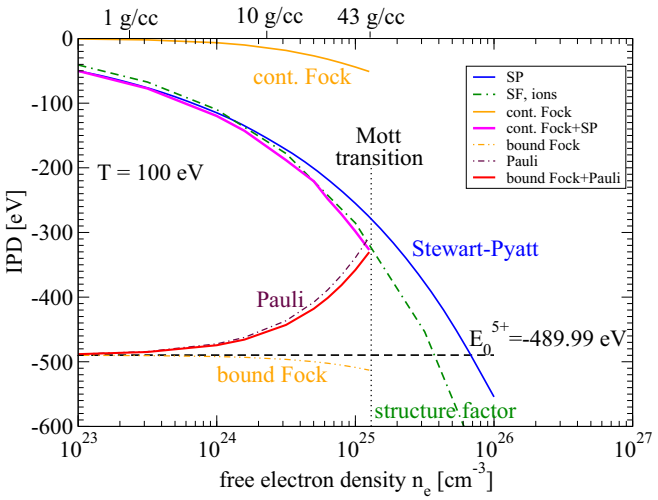

FIG. 1. Ionization potential depression (IPD) of C^{5+} as function of the free-electron density n_e at fixed temperature $T=100$ eV. The Fock shift of the continuum edge (cont. Fock), Eq. (20) at $p=0$, together with the Stewart-Pyatt (SP) IPD (2) yields the shift of the continuum (cont. Fock+SP). For the ion C^{5+} in its ground state, the Pauli shift Eq. (32) (Pauli) and the bound-state Fock shift Eq. (30) (bound Fock) as well as the sum of both (bound Fock+Pauli) are presented. For comparison, the IPD obtained from the ionic structure factor shift of the continuum (SF, ions) as improvement of the SP model [20] is also shown. The Mott transition is predicted at $n_e=1.3\times10^{25}$ cm^{-3}. Upper scale: Carbon mass density.

Compared to the Fock shift $\Delta_e^{\rm Fock}(0)$ of the continuum edge, the bound-state Fock shift $\Delta_0^{\rm bound,\,Fock}$ is determined by the momentum-dependent Fock shift Eq. (20). The latter becomes smaller near the Fermi momentum, so that the bound-state Fock shift is also smaller compared to the Fock shift of the continuum edge.

The Pauli blocking shift is given by

$$\Delta_0^{\rm bound,\,Pauli} = -\sum_{p,q} \phi_0(p) f_e(p) V_{C^{6+},e}(q) \phi_0(\mathbf{p}+\mathbf{q}) = \frac{Ze^2}{4\pi\epsilon_0}\frac{16a_Z^2}{\pi}\int_0^\infty f_e(p)\frac{p^2dp}{\left(1+a_Z^2p^2\right)^3}, \quad (32)$$

which becomes at $T=0$

$$\Delta_{0,T=0}^{\rm bound,\,Pauli} = \frac{Ze^2}{4\pi\epsilon_0}\frac{2}{\pi a_Z}\left[\frac{a_Z p_F\left(a_Z^2p_F^2-1\right)}{\left(a_Z^2p_F^2+1\right)^2}+\arctan(a_Z p_F)\right]. \quad (33)$$

At finite temperatures, the integrals in Eqs. (30) and (32) are calculated numerically. Note that both effects, the Fock shift and the Pauli shift, have different sign and compete partially. Calculations are shown in Sec. III; see Fig. 1.

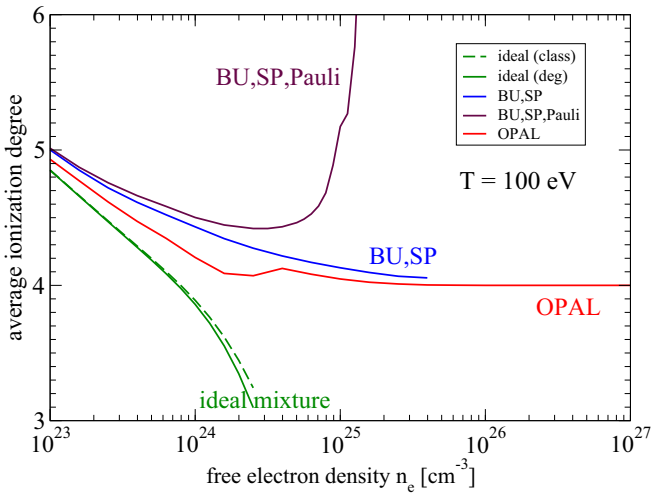

FIG. 2. Average ionization degree $\bar{Z}$ of carbon as function of the free-electron density n_e for temperature $T = 100$ eV. Ideal mixture with electron treated classically (ideal,class) and as Fermi gas (ideal, deg), OPAL and Stewart/Pyatt (BU,SP) are also shown. BU denotes the use of the Beth-Uhlenbeck Eqs. (15) and (18) for the intrinsic partition function, SP the Stewart-Pyatt contribution Eq. (2). In addition the SP Eq. (2), the full IPD (BU,SP,Pauli) contains the Fock shift of the continuum Eq. (20) at $p = 0$ as well as the Fock shift of the bound-state Eq. (30) and the Pauli blocking Eq. (32).

III. RESULTS FOR DEGENERATE PLASMAS

A. Pauli blocking in carbon plasmas

We present results for the ionization degree of carbon plasmas in the WDM regime. The composition of the carbon plasma for given mass density and temperature is determined by the abundances of ions C^{i+} with different charge $Z_i e$, $Z_i = 0, 1, \ldots, 6$ (including the neutral atom). The composition of the partially ionized plasma (PIP) is described by the partial densities, Eq. (6), obtained in Sec. II B.

To start with we briefly recall the ideal PIP model neglecting any medium effects. This approximation is applicable in the low-density region where we have nearly free motion of the constituents of the PIP. In this limiting case, we consider noninteracting ions C^{i+} in its ground state and bound excited states. The electrons which are not bound to ions are considered as free electrons. The densities of the different components of the plasma are connected by the neutrality condition $\sum_i Z_i n_i = n_e$. The ionization energies I_i necessary to separate an electron from the carbon ion C^{i+} are known ($I_0^{(0)} = 11.2603$ eV, $I_1^{(0)} = 24.3833$ eV, $I_2^{(0)} = 47.8878$ eV, $I_3^{(0)} = 64.4939$ eV, $I_4^{(0)} = 392.087$ eV, $I_5^{(0)} = 489.9933$ eV). In addition, the excited states must be included, data can be found in Ref. [39]. To have convergent results, the Planck-Larkin Eq. (A6) is used for the intrinsic partition function. The solution of the Saha equations for the partial densities of different ions (ground state and excited state) gives the average ionization degree $\bar{Z}$ and the corresponding free-electron density $n_e = \bar{Z} n_C$ as function of the temperature T and the density of carbon nuclei n_C in the charge-neutral equilibrium state. Results for $\bar{Z}$ are shown below in Fig. 2 ("ideal mixture") for $T_1 = 100$ eV as function of n_e. The convergent Planck-Larkin intrinsic partition functions are [39] $\sigma_5^{\rm PL}(T_1) = 266.241$, $\sigma_4^{\rm PL}(T_1) = 54.197$, $\sigma_3^{\rm PL}(T_1) = 1.6889$, $\sigma_2^{\rm PL}(T_1) = 1.2345$, $\sigma_1^{\rm PL}(T_1) = 0.5459$, and $\sigma_0^{\rm PL}(T_1) = 0.08885$. For the ideal electron gas, the classical approximation has been compared to the ideal Fermi gas Eq. (4), but effects of degeneracy are small in the region of density and temperature considered there. However, an ideal, noninteracting plasma model with occasional reactions to establish chemical equilibrium is not appropriate for a dense plasma where interactions have to be taken into account.

We now discuss the in-medium effects such as Debye screening and its improvements by SP and SF as well as Pauli blocking and Fock shifts, which determine the quasiparticle energies in the dense plasma for the hydrogenlike ion C^{5+}. Results for the different contributions to the in-medium shifts are shown for $T = 100$ eV as function of the free-electron density n_e in Fig. 1. For the ground state of C^{5+}, the ionization potential in free space is $I_5^{(0)} = 489.9933$ eV. It is reduced by screening. Improving the Debye result for the correlation part, the SP approximation Eq. (2) gives a Mott density $n_{e,\rm Mott}^{\rm SP} = 6.89 \times 10^{25}$ cm^{-3} where the bound state merges with the continuum. Within the quantum statistical approach [20] determined by the ionic structure factor ("SF, ions"), the IPD is larger, see Fig. 1. The corresponding Mott density for $T = 100$ eV follows as $n_{e,\rm Mott}^{\rm SF} = 3.78 \times 10^{25}$ cm^{-3}.

With increasing density, the effects of degeneracy of the electron subsystem become of increasing importance. Whereas the Fock shifts $\Delta_e^{\rm Fock}(0)$ Eq. (20) of the continuum edge and, even more, the Fock shift of the bound-state Eq. (30) remain small, the Pauli blocking Eq. (32) becomes relevant for the dissolution of the bound state. Taking into account all effects of degeneracy, the Mott density is further reduced and the value $n_{e,\rm Mott}^{\rm deg} = 1.28 \times 10^{25}$ cm^{-3} is obtained. Note that the condition $\Theta = 1$, where the free-electron system becomes degenerate, for a temperature of $T = 100$ eV is satisfied at

an electron density $n_e^{\rm deg} = 4 \times 10^{24}$ cm^{-3}, which corresponds to a mass density of 20 g cm^{-3} for a carbon plasma as mentioned in the Introduction. Above this density, degeneracy effects, in particular Pauli blocking and Fock shifts, have to be considered. Similar results are obtained also for the other ionization states of carbon.

In conclusion, the ionization potential $I_i = I_i^{(0)} + \Delta_i^{\rm corr} + \Delta_i^{\rm deg}$ contains contributions due to correlations as well as degeneracy. At low densities the composition of the partially ionized plasma is well described using the IPD in Debye approximation or its improved versions, the semi-empirical SP or the quantum statistical SF approaches, which also include strong correlation effects. The effects of degeneracy, in particular Pauli blocking, become of relevance in the region of higher densities where the free-electron system is degenerate, $\Theta \leqslant 1$. The region, where the plasma is nearly fully ionized, is strongly modified if Pauli blocking is taken into account.

To demonstrate the effect of Pauli blocking on $\bar{Z}$, we performed calculations of the ionization degree of carbon as function of the free-electron density at a fixed temperature $T = 100$ eV, see Fig. 2. Arbitrary ionization stages Z_i of carbon as well as excited states according to the NIST tables [39] have been included. For the contributions of free and bound electrons to the density, we use the definition Eq. (15) but neglect the contribution of scattering states Eq. (18). The term -1 in the bound-state contribution makes this part continuous near the Mott density where the bound state disappears. It compensates partly the contribution of scattering states according to the Levinson theorem. Together with the extraction of the Born approximation, which is transferred to the quasiparticle shift [28,30], we assume that the continuum contribution to the correlated density (second term of the right-hand side of Eq. (15) becomes small and can be neglected. For further discussion, see Sec. IV.

The calculation of the intrinsic partition functions and the corresponding partial densities has been performed in a self-consistent way. Starting from the given T and the number density n_C of carbon nuclei, the free-electron density n_e, the electron chemical potential, and the shifts are calculated, adopting a value $\bar{Z}$ of the ionization degree. The Fock and Pauli shifts are immediately calculated with the free-electron density. For the Stewart-Pyatt shift Eq. (2) we need, in addition to the free-electron density, also the screening parameter κ Eqs. (1) and (19), where $\sum_i Z_i^2 n_i \approx \bar{Z} \sum_i Z_i n_i$ has been used. Choosing the density of ions C^{6+}, the partial densities of all ion states are calculated solving the Saha Eqs. (8) and (10) with these shifts, as well as the free-electron density and the ionization degree. Then, the self-consistent solution for $\bar{Z}$ was found. After that, the density of ions C^{6+} is changed to reproduce the given carbon number density. Finally, κ is calculated consistently with the partial densities according Eqs. (1) and (19). As a result, for given T and n_C, we found the densities of all components of the partially ionized plasma, as well as the ionization degree $\bar{Z}$.

Neglecting all in-medium effects, the approximation of an ideal mixture discussed above becomes increasingly worse when n_e exceeds the value 10^{23} cm^{-3}. The account of IPD according to SP (denoted as "BU, SP" in Fig. 2) gives an ionization degree of about $\bar{Z} = 4$ even at very high densities. This is also obtained from OPAL [22]. These values are used

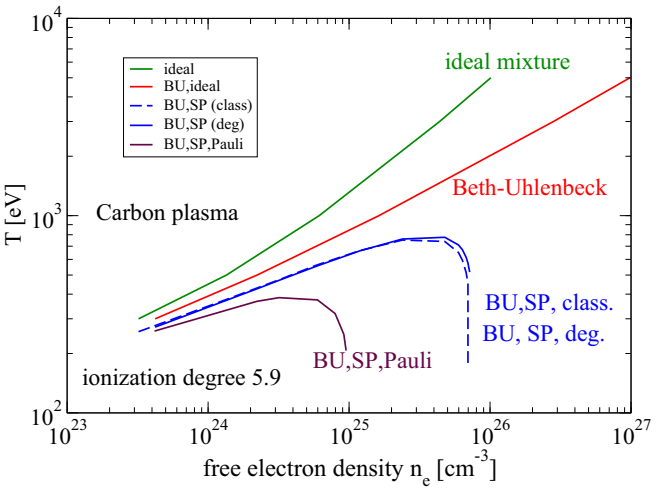

FIG. 3. Temperatures for the ionization degree of $\bar{Z} = 5.9$ (isoionization lines) using different approximations for the IPD. $T_{5.9}^{\rm ideal}$ for the ideal mixture is compared with the ideal Beth-Uhlenbeck expression $T_{5.9}^{\rm BU,ideal}$ Eqs. (15) and (18), neglecting any medium effects. The account of the correlation shifts for the IPD, given by the Stewart-Pyatt model Eq. (2), yields the graph $T_{5.9}^{\rm BU,SP,class}$ for a classical free-electron gas or $T_{5.9}^{\rm BU,SP,deg}$ for the Fermi gas. In addition to the SP shift, the full IPD contains the Fock shift of the continuum Eq. (20), $p = 0$, as well as the Fock shift of the bound-state Eq. (30) and the Pauli blocking Eq. (32). It gives the graph $T_{5.9}^{\rm BU,SP,Pauli}$.

when measurements have been compared to theory [40,41]; see Sec. III B. More recent quantum statistical approaches [20] which relate the IPD to the ionic structure factor give a slightly higher value for the ionization degree not shown here.

The ionization degree $\bar{Z}$ is found to be further increased if degeneracy effects, the Fock shift and the Pauli blocking, are taken into account. The corresponding ionization degree is shown in Fig. 2 (denoted as "BU, SP, Pauli"). The value $\bar{Z} = 6$ appears for densities larger than the Mott density $n_{e,\rm Mott}^{\rm deg} = 1.29 \times 10^{25}$ cm^{-3}, i.e., at a much lower density than predicted by the SP model. The Mott effect gives full ionization if all bound states merge with the continuum of delocalized electron states. This is clearly seen using the virial form Eq. (15) of the intrinsic partition function, if only bound states are taken into account.

Of interest are the properties of WDM at high densities where the plasma becomes highly ionized. Because there is no sharp transition to the fully ionized plasma, we consider the value $\bar{Z} = 5.9$ for the ionization degree as a nearly fully ionized carbon plasma with only 10 percent hydrogen-like carbon ions. This concentration is decreasing with increasing temperature. In Fig. 3, we show graphs of constant ionization degree $\bar{Z} = 5.9$ (isoionization line) in the phase diagram T, n_C (or T, n_e with the relation $n_e = 5.9\, n_C$) for which the plasma is nearly fully ionized. Isoionization lines with $\bar{Z} = 5.9$ in carbon are calculated for different approximations.

For an ideal mixture of noninteracting components in chemical equilibrium, treating the electrons classically, the temperature $T_{\bar{Z}=5.9}^{\rm ideal}(n_e)$ increases with increasing density. This behavior is only slightly shifted to lower temperatures if the

TABLE I. Ionization degree $\bar{Z}$ of carbon at WDM conditions. The treatment within the Stewart-Pyatt (index SP) approach is compared to a treatment where also the effects of degeneracy (index SP, deg) are taken into account. In addition to the ionization degrees in the respective approaches also the SP contribution $\Delta I^{5,\mathrm{SP}}_{\mathrm{SP,\,deg}}$ to the shift of the ionization potential as well as the contribution owing to the effects of degeneracy $\Delta I^{5,\mathrm{deg}}_{\mathrm{SP,\,deg}}$ are given, which contains in addition to the Fock shifts Eqs. (20) and (30) also the Pauli blocking term Eq. (32). $\Theta = T/T_{\mathrm{Fermi}}$ is the electron degeneracy parameter Eq. (3). For $T = 8$ eV (strong degeneracy), the Mott condition Eq. (18) with $I_{i,\gamma,v} + E_F > 0$ has been used. The different contributions for the energy shifts for the bottom line are visualized in Fig. 1 for $n_e \approx 10^{25}$ cm^{-3}, just before the Mott transition.

Material	T [eV]	ρ [g cm^{-3}]	n_C [cm^{-3}]	$\bar{Z}_{\mathrm{exp}}$	$\bar{Z}_{\mathrm{SP}}$	$\Delta I^{5}_{\mathrm{SP}}$ [eV]	$\bar{Z}_{\mathrm{SP,\,deg}}$	$\Delta I^{5,\mathrm{SP}}_{\mathrm{SP,\,deg}}$ [eV]	$\Delta I^{5,\mathrm{deg}}_{\mathrm{SP,\,deg}}$ [eV]	Θ
CH [40]	8 ± 1	4.5 ± 0.5	2.08×10^{23}	4 ± 0.5	2.04	90.47	4.0	114.02	54.45	0.213
CH [41]	86	6.74	3.12×10^{23}	4.9	4.18	125.8	4.26	126.74	38.53	1.69
C	8	4.15	2.08×10^{23}	—	2.88	101.7	4.0	113.9	46.9	0.247
C	86	6.22	3.12×10^{23}	—	4.21	125.7	4.29	126.6	31.8	1.94
C	100	40	2.01×10^{24}	—	4.14	236.9	5.19	258.1	182.4	0.574

IPD according to SP Eq. (2) is included. Two corrections can immediately be done: the quantum description of the electron gas according to Eq. (4) which determines the relation between density and chemical potential necessary for the chemical equilibrium Eq. (10), and the term -1 occurring in the Beth-Uhlenbeck Eq. (15). Neglecting the IPD, the bound states are not dissolved with increasing density. As compared to the "ideal" curve $T^{\mathrm{ideal}}_{5.9}$, the more consistent $T^{\mathrm{BU,ideal}}_{5.9}$ which contains the Beth-Uhlenbeck form Eq. (18) of the intrinsic partition function, is shifted to lower values, but also increases monotonically with density.

According to Eq. (18), only bound states are taken into account, i.e., the ionization potential of the bound state must be positive. The Mott effect becomes visible if the IPD compensates the vacuum ionization potential $I^{(0)}_i$. The corresponding $T^{\mathrm{BU,SP,deg.}}_{5.9}$ in Fig. 3 using the Stewart-Pyatt approximation for the IPD shows a strong deviation from the other curves. (Note that the classical result for the electron chemical potential used for $T^{\mathrm{BU,SP,class.}}_{5.9}$ gives only small deviations.) In particular, for electron densities higher than the Mott density $n^{\mathrm{SP}}_{e,\mathrm{Mott}}$ given above, all electrons are free, and the isoionization curve for $T^{\mathrm{BU,SP,deg}}_{5.9}$ abruptly goes to zero. Even larger is the effect if exchange terms, in particular Pauli blocking, are included. The curve $T^{\mathrm{BU,SP,Pauli}}_{5.9}$ in Fig. 3 indicates that the region of full ionization is reached already at the Mott density $n^{\mathrm{deg}}_{e,\mathrm{Mott}}$ consistent with the results shown in Fig. 1.

The strong influence of the IPD on the onset of full ionization, where $T_{5.9}$ is shifted to lower temperatures if Pauli blocking is taken into account, leads to higher values for the average degree of ionization $\bar{Z}$. Higher values of $\bar{Z}$ have been observed in experiments [40,41] when comparing to OPAL [22], which neglects degeneracy effects such as bound-state Pauli blocking.

B. Comparison to other approaches and experiments

The ionization degree of carbon at $T = 100$ eV has also been considered in Ref. [42]. The calculations used an average atom model with different boundary conditions to mimic a band width, and the bound-state contribution was defined by the part of the band below the energy of the continuum edge. Qualitatively, the results are similar to the results for the ionization degree shown in Fig. 2, denoted as "BU, SP, Pauli," and full ionization is predicted near the Mott density. Similar calculations have been performed recently for lower temperatures and densities in Ref. [43]. It is not clear to which extent correlation and degeneracy effects obtained from a systematic quantum statistical approach are already contained in those semiempirical approaches.

Recently, WDM has been treated successfully within DFT approaches, see, e.g., Refs. [44,45]. Calculations for carbon plasmas [26,53] have been performed, where results for the pressure and the internal energy are obtained. As an approach that is very appropriate to investigate condensed matter, the DFT formalism also describes Pauli blocking and the formation of band structures. However, composition, ionization degree $\bar{Z}$, and IPD are not directly accessible within this approach; see also Sec. IV.

Carbon ionization $\bar{Z}$ at WDM conditions was measured in experiments [40,41] with CH using x-ray Thomson scattering; see Table I. The observed ionization degree of carbon ions was higher than the predictions of SP. In Ref. [41], the mean charge $\bar{Z} = 4.9$ was measured at density 6.7 g/cm^3 and $T = 86$ eV, which is higher than the prediction $\bar{Z} = 4.18$ from SP. This discrepancy is only partly resolved using the SF approach [20] for this two-component plasma in the simulations where a value $\bar{Z} = 4.79$ has been reported. In contrast to pure carbon plasmas, ionic structure factors S_{CC}, S_{CH}, S_{HH} for the different components have to be taken into account, and an increase of the ionization degree was obtained. Further work is in progress [36].

Taking Pauli blocking into account leads to a further increase of the ionization degree. We show some results for the energy shifts and ionization degree for pure carbon plasmas as well as for CH plasmas in Table I. The temperatures T and mass densities ρ are in accordance with the parameter values given in the experiments of Refs. [40,41]. The number densities n_C of carbon atoms are calculated with the molar mass number 12 for C and 13 for CH. We treat the CH plasma in a simple approximation where the H component is fully dissociated into a proton and an electron. Both the additional proton and electron will change the screening parameter κ by adding the proton to the ionic contribution in Eq. (1), and it will change the free-electron density as $n_e = (\bar{Z} + 1)n_C$. The influence of the additional electron on the chemical equilibrium between the different carbon ions, as expressed

by the coupled Saha equations, is complex and is calculated self-consistently. The increase of the screening parameter κ leads to an increase of the ionization degree. However, the additional electrons owing to the ionized H atoms can partially enter the ionic bound states as described by the Saha equations. This leads to a decrease of the ionization degree, because more bound electrons appear and the average charge of carbon ions is decreasing. To compare CH plasmas to C plasmas, a calculation for pure carbon plasmas with identical T and carbon number density n_C is shown in Table I. In addition, we chose $T = 100$ eV and $\rho = 40$ g/cm^3, which is of interest for future experiments.

The composition was calculated with the generalized Beth-Uhlenbeck Eq. (15) where the in-medium bound-state energies are shifted. With the Mott condition $I_{i,\gamma,\nu} > 0$, see Eq. (18), the contribution of scattering states is neglected. Here, $I_{i,\gamma,\nu} = E_{i,\gamma,\nu} - E_{i,\,\mathrm{cont}}$ denotes the ionization energy of the ion a_i in the state γ (channel, e.g., angular momentum) and excitation ν, and $E_{i,\,\mathrm{cont}}$ is the continuum edge of the ion a_{i+1} and the electron. For the lowest temperature, in the case of strong degeneracy, contributions of scattering states are of relevance because bound-state-like correlations exist for energies below the Fermi energy $E_F = \hbar^2 p_F^2/2m_e$. As shown in Ref. [32], for strong degeneracy the Mott condition $I_{i,\gamma,\nu} + E_F > 0$ can be used. The shift of the ionization potential $\Delta I^{5,\mathrm{SP}}_{\mathrm{SP,\,deg}}$ is the IPD according to SP for the ion C^{5+}; see Fig. 1. The additional shift owing to the effects of degeneracy is denoted as $\Delta I^{5,\mathrm{deg}}_{\mathrm{SP,\,deg}} = -\Delta^{\mathrm{Fock}}_e + \Delta^{\mathrm{bound,Pauli}} + \Delta^{\mathrm{bound,Fock}}$ which contains in addition to the Fock shifts Eqs. (20) and (30) also the Pauli blocking term Eq. (32). The total IPD when taking degeneracy effects into account is the sum of these two contributions: $\Delta I^{5}_{\mathrm{SP,\,deg}} = \Delta I^{5,\mathrm{SP}}_{\mathrm{SP,\,deg}} + \Delta I^{5,\mathrm{deg}}_{\mathrm{SP,\,deg}}$. The index "SP" refers to a calculation where only the SP term for the IPD is considered, the index "SP,deg" refers to a calculation where both, SP and degeneracy, are taken into account for IPD. For the latter case, the electron degeneracy parameter $\Theta = T/T_{\mathrm{Fermi}}$ Eq. (3) is also given.

As shown in Table I, taking the effects of degeneracy into account (in particular Pauli blocking), leads to an increase of the ionization degree $\bar{Z}$. This effect is marginal for nondegenerate plasmas ($\Theta > 1$) but becomes important in degenerate plasmas ($\Theta \ll 1$). The calculations for CH plasmas and C plasmas with corresponding plasma parameters are not very different. With respect to the experimental data, the inclusion of degeneracy effects gives better results. Our exploratory considerations should be completed by including further contributions such as the structure factor effects [20] or the polarization of the ion core. A more detailed description will be given in forthcoming work. In addition, the range of validity of the perturbation theory must be checked.

Until now, experimental data show higher ionization degrees compared to the usually used SP approximation or the OPAL data tables. The Pauli blocking discussed in our work can be considered as a possible mechanism in degenerate plasmas which contributes to the increase of the ionization degree. Experiments for pure carbon plasmas at very high densities up to 40 g/cm^3 are in preparation at the NIF. We expect that these experiments will show the relevance of the Pauli blocking effect as a mechanism to increase the charge state of carbon ions in degenerate WDM states.

IV. CONCLUSIONS

The Pauli blocking has to be taken into account for extreme high-density WDM when the electrons are strongly degenerate. This exchange effect seems to be essential for the appearance of high ionization degrees as compared to standard approaches considering only screening effects, e.g., SP used for opacity tables like OPAL [8,13–15,40,41,46–49]. Within the many-body approach described in the present work, further effects such as the polarization shift of the bound states can be considered, and the correlation (Montroll-Ward) contribution to the electron self-energy can be improved taking higher-order Feynman diagrams into account. For instance, ion correlations expressed by the dynamical ionic structure factor have been considered recently [20]. Another interesting effect is that Pauli blocking is only approximately described by the ideal Fermi distribution in Eq. (27). In general, correlations and bound-state formation also contribute to phase space occupation so that it deviates from the ideal Fermi distribution; see Ref. [23]. In addition, the perturbative treatment of Pauli blocking is improved if the full solution of the in-medium Schrödinger Eq. (27) is worked out; see also Refs. [3,19,37].

The concept of the ionization degree or plasma composition is a useful approach to PIP but has to be used with care, in particular with respect to the inclusion of scattering states. The ordinary chemical picture which considers the PIP as a mixture of different components, the free particles as well as the bound clusters, neglects the correlations between these components. The so-called physical picture, where only the "elementary" constituents (electrons and nuclei) and their interaction are considered, provides a consistent description of WDM. The drawbacks of the ordinary chemical picture are avoided if spectral functions are considered, which are well defined at arbitrary densities. Single-quasiparticle states and bound states are approximations for the spectral functions where the energy levels are shifted and broadened because of the interaction with the plasma environment. In particular, the broadening of energy levels (Inglis-Teller effect [50,51]) has to be considered if the signatures of bound states as separate peaks in the spectra disappear.

A challenge is the use of density-functional theory [9–12] where the single-particle density of states is evaluated. Assuming that the broadening of the bands is less important for the integral over the spectral function, see Eq. (11), the shifts of the bands can be compared with the level shifts in our approach. Work in this direction is in progress [52], see also Ref. [53] where orbital-free molecular dynamics is performed, and the sensitivity of the equations of state, obtained there, to the choice of exchange-correlation functionals is investigated. Correct results for thermodynamic quantities are also available from PIMC calculations [16] in the high-temperature region where the difficulties using a nodal structure are less relevant. Controversies such as the treatment of strongly degenerate systems [26,54] where $\mu_e \approx E_F$ may be resolved within the quantum statistical approach, considering the contribution of scattering phase shifts; see Ref. [55]. For the strongly degenerate electron gas, bound-state-like contributions do not disappear if the bound state merges with the continuum of scattering states. At zero temperature, correlations in the continuum give a contribution to the

correlated density until the bound state merges with the Fermi energy.

The full solution of the quantum statistical approach, including the contribution of scattering states, is needed to obtain a consistent description of physical properties of the partially ionized plasma [32]. This is possible in the "physical" picture, i.e., the solution of the many-body problem for interacting electrons and nuclei. The ordinary "chemical" picture is improved using the quasiparticle concept. Instead of free particles, single-quasiparticle states are introduced which contain already contributions of interaction in mean-field approximation. In addition, correlations are defined which contain not only the in-medium bound states but also the correlations in the continuum.

The Pauli blocking is a quantum effect based on the antisymmetrization of the many-electron wave function. It is only approximately described by an empirical potential for the interaction of bound states. A consistent description is given within the physical picture, solving the few-particle in-medium Schrödinger equation (so-called Bethe-Salpeter equation) which contains the phase-space occupation in the interaction term. The expression for an uncorrelated medium Eq. (26) given by the Fermi distribution function should be improved taking correlations in the medium into account; see Refs. [56]. In conclusion, the Pauli blocking is essential to describe the dissolution of bound states and the increase of the ionization degree at high densities when the WDM is strongly degenerate.

ACKNOWLEDGMENTS

The work of T.D. was performed under the auspices of the U.S. Department of Energy by Lawrence Livermore National Laboratory under Contract No. DE-AC52-07NA27344 and supported by Laboratory Directed Research and Development (LDRD) Grant No. 18-ERD-033. D.B. and G.R. acknowledge partial support from the National Research Nuclear University (MEPhI) in the framework of the Russian Academic Excellence Project under Contract No. 02.a03.21.0005. D.B. was supported by the Russian Science Foundation under Grant No. 117-12-01427 for his contributions to Sections I, II.A and II.B. R.R. acknowledges support from the Deutsche Forschungsgemeinschaft (DFG) via the research unit FOR 2440.

APPENDIX: EXACT RELATIONS FOR THE SECOND VIRIAL COEFFICIENT AND THE PLANCK-LARKIN EXPRESSION FOR THE INTRINSIC PARTITION FUNCTION

According to Beth and Uhlenbeck [27], the contribution of correlations from the channel γ to the intrinsic partition function is expressed in terms of the bound-state energies $E_{i,\gamma,\nu}$ and the scattering phase shifts $\delta_{i,\gamma}(E)$,

$$\sigma_{i,\gamma}(T) = \sum_{\nu}^{\text{bound}} e^{-\beta E_{i,\gamma,\nu}} + \int_0^\infty \frac{dE}{\pi} e^{-\beta E} \frac{d}{dE}\delta_{i,\gamma}(E). \quad \text{(A1)}$$

After integration by parts and using the Levinson theorem [57,58], the alternative expression, Eq. (9), is obtained. A remarkable property of both relations, Eqs. (9) and (A1), is that they contain only properties which can be measured but not the interaction potential.

However, in the case of Coulomb interactions, scattering phase shifts can not be defined in the standard way because of the long-range character of the Coulomb potential. This problem has been investigated in plasma physics for a long time; see Refs. [3,4,22,59]. We give here a result for the intrinsic partition function of hydrogenlike ions. Using the abbreviations $\xi_{ab} = -e_a e_b/(k_B T \lambda_{ab})$, $\lambda_{ab} = \hbar/\sqrt{2 m_{ab} k_B T}$, $m_{ab} = m_a m_b/(m_a + m_b)$, we have up to the second order of the fugacity $z_a = \exp \beta\mu_a$ the exact result (see, e.g., Refs. [3,60])

$$n_a = z_a - \frac{\kappa e^2}{2} - \sum_b z_b \left\{ -\frac{\pi}{3}(\beta e_a e_b)^3 \ln(\kappa\lambda_{ab}) + \frac{\pi}{2}\beta^3 e_a^2 e_b^4 - 2\pi\lambda_{ab}^3 \left[Q_1(\xi_{ab}) \pm \delta_{ab} \frac{(-1)^{s_a}}{s_a+1} Q_2(\xi_{ab}) \right] \right\} + \mathcal{O}\left(z_a^{3/2} \ln z_a\right). \quad \text{(A2)}$$

Here, the direct terms are described by the function

$$Q_1(\xi) = -\frac{\sqrt{\pi}}{8}\xi^2 - \frac{\xi^3}{6}\left(\frac{C}{2} + \ln 3 - \frac{1}{2}\right) + \sum_{p=4} \frac{\sqrt{\pi}\zeta(p-2)}{\Gamma(p/2+1)} \times \left(\frac{\xi}{2}\right)^p, \quad \text{(A3)}$$

with the Riemann zeta function $\zeta(x)$, the Γ function $\Gamma(x)$, and $C = 0.5772$ being the Euler constant. The exchange term ($+$ for fermions, $-$ for bosons) reads

$$Q_2(\xi) = \frac{\sqrt{\pi}}{4} + \frac{\xi}{2} + \sqrt{\pi}\ln 2\left(\frac{\xi}{2}\right)^2 + \frac{\pi^2}{9}\left(\frac{\xi}{2}\right)^3 + \sum_{p=4} \frac{\sqrt{\pi}(1-2^{2-p})\zeta(p-1)}{\Gamma(p/2+1)}\left(\frac{\xi}{2}\right)^p. \quad \text{(A4)}$$

We separate the electron-ion bound-state contribution [with the step function $\theta(\xi)$ according to Eq. (18)]

$$\begin{aligned} Q_1(\xi) &= 2\sqrt{\pi}[\sigma^{\text{PL,bound}}(T) + \sigma^{\text{PL,cont}}(T)] \\ &= 2\sqrt{\pi}\sigma^{\text{PL,bound}}(T)\theta(\xi) - \text{sign}(\xi) Q_1(-\xi) \\ &\quad - \tfrac{1}{4}\sqrt{\pi}\theta(\xi)\xi^2, \end{aligned} \quad \text{(A5)}$$

with the Planck-Larkin bound-state partition function

$$\sigma^{\text{PL, bound}}(T) = \sum_{n=1}^{\infty} 2n^2[e^{-\beta E_n} - 1 + \beta E_n], \quad \text{(A6)}$$

where n runs over the intrinsic quantum numbers (including spin) of all bound states, $E_n = -e^2/(4\pi\epsilon_0 a_B n^2)$. The total intrinsic partition function $\sigma^{\text{PL,bound}}(T) + \sigma^{\text{PL,cont}}(T)$ is divided into a bound-state part and a continuum part both of which are convergent. As a peculiarity of the long-range Coulomb interaction where scattering phase shifts cannot be introduced in the standard way, instead of Eqs. (9) and (A1) the definition Eq. (A6) can be used to define a convergent bound-state part of the intrinsic partition function.

To calculate the plasma composition, usually only the bound-state part of the intrinsic partition function is taken, and the continuum contributions are neglected. Although Eqs. (9), (A1), and (A6) for the intrinsic partition function $\sigma_i(T)$ give

exact results for the second virial coefficient, the subdivision into the contribution of bound states and scattering states is different and the corresponding definition of composition and ionization degree is model-dependent. In this work, another approach is proposed. Instead of free electrons, we consider the quasiparticle contribution to the spectral function, and instead of electrons bound in ions we consider the correlated part of the density, as shown with Eq. (15). This approach is based on a cluster decomposition of the self-energy [29] and allows to include also the contribution of resonances.

[1] R. W. Lee, D. Kalantar, and J. Molitoris, *Warm Dense Matter: An Overview*, in Livemore, http://e-reports-ext.llnl.gov/pdf/307164.pdf (2004).

[2] N. F. Mott, Rev. Mod. Phys. **40**, 677 (1968); R. Redmer, F. Hensel, and B. Holst (eds.), *Metal-to-Nonmetal Transitions*, Springer Series in Materials Science, Vol. 132. (Springer-Verlag, Berlin/Heidelberg, 2010).

[3] W.-D. Kraeft, D. Kremp, W. Ebeling, and G. Röpke, *Quantum Statistics of Charged Particle Systems* (Akademie-Verlag, Berlin, 1986).

[4] D. Kremp, M. Schlanges, and W.-D. Kraeft, *Quantum Statistics of Nonideal Plasmas* (Springer-Verlag, Berlin/Heidelberg, 2005).

[5] G. Zimmerman and R. More, JQSRT **23**, 517 (1980).

[6] G. Ecker and W. Kröll, Phys. Fluids **6**, 62 (1963).

[7] J. C. Stewart and K. D. Pyatt Jr., Astrophys. J. **144**, 1203 (1966).

[8] D. J. Hoarty *et al.*, Phys. Rev. Lett. **110**, 265003 (2013).

[9] S. M. Vinko *et al.*, Nature **482**, 59 (2012).

[10] S. M. Vinko, O. Ciricosta, and J. S. Wark, Nat. Commun. **5**, 3533 (2014).

[11] S. M. Vinko *et al.*, Nat. Commun. **6**, 6397 (2015).

[12] M. F. Kasim, J. S. Wark, and S. M. Vinko, Sci. Rep. **8**, 6276 (2018).

[13] O. Ciricosta *et al.*, Phys. Rev. Lett. **109**, 065002 (2012).

[14] O. Ciricosta *et al.*, Nat. Commun. **7**, 11713 (2016).

[15] B. J. B. Crowley, High Energy Density Phys. **13**, 84 (2014).

[16] K. P. Driver, F. Soubiran, and B. Militzer, Phys. Rev. E **97**, 063207 (2018); K. P. Driver and B. Militzer, Phys. Rev. Lett. **108**, 115502 (2012); S. Zhang, K. P. Driver, F. Soubiran, and B. Militzer, Phys. Rev. E **96**, 013204 (2017).

[17] T. Dornheim, S. Groth, and M. Bonitz, Phys. Rep. **744**, 1 (2018).

[18] F. Graziani, M. P. Desjarlais, R. Redmer, and S. B. Trickey (eds.), *Frontiers and Challenges in Warm Dense Matter*, Vol. 96 (Springer, Cham, 2014).

[19] J. Seidel, S. Arndt, and W.-D. Kraeft, Phys. Rev. E **52**, 5387 (1995).

[20] C. Lin, G. Röpke, W. D. Kraeft, and H. Reinholz, Phys. Rev. E **96**, 013202 (2017).

[21] D. Kraus *et al.*, J. Phys.: Conf. Ser. **717**, 012067 (2016); T. Döppner *et al.*, Phys. Rev. Lett. **121**, 025001 (2018); D. Kraus *et al.*, Plasma Phys. Control. Fusion **61**, 014015 (2019).

[22] F. J. Rogers, F. J. Swenson, and C. A. Iglesias, Astrophys. J. **456**, 902 (1996).

[23] G. Röpke, Phys. Rev. C **79**, 014002 (2009); Nucl. Phys. A **867**, 66 (2011); Phys. Rev. C **92**, 054001 (2015).

[24] G. Röpke, D. Blaschke and H. Schulz, Phys. Rev. D **34**, 3499 (1986); D. Blaschke, M. Buballa, A. Dubinin, G. Röpke, and D. Zablocki, Ann. Phys. **348**, 228 (2014).

[25] W. Ebeling, D. Blaschke, R. Redmer, H. Reinholz, and G. Röpke, J. Phys. A: Math. Theor. **42**, 214033 (2009).

[26] S. X. Hu, Phys. Rev. Lett. **119**, 065001 (2017); C. A. Iglesias and P. A. Sterne, *ibid.* **120**, 119501 (2018); S. X. Hu, *ibid.* **120**, 119502 (2018).

[27] E. Beth and G. Uhlenbeck, Physica **4**, 915 (1937).

[28] R. Zimmermann and H. Stolz, Phys. Stat. Sol. (b) **131**, 151 (1985).

[29] G. Röpke, L. Münchow, and H. Schulz, Nucl. Phys. A **379**, 536 (1982).

[30] M. Schmidt, G. Röpke, and H. Schulz, Ann. Phys. **202**, 57 (1990).

[31] G. Röpke, N.-U. Bastian, D. Blaschke, T. Klähn, S. Typel, and H. H. Wolter, Nucl. Phys. A **897**, 70 (2013).

[32] G. Röpke, arXiv:1901.08044 [Contrib. Plasma Phys. (to be published)].

[33] J. Chihara, J. Phys: Condens. Matter **12**, 231 (2000).

[34] G. Gregori, S. H. Glenzer, K. B. Fournier, K. M. Campbell, E. L. Dewald, O. S. Jones, J. H. Hammer, S. B. Hansen, R. J. Wallace, and O. L. Landen, Phys. Rev. Lett. **101**, 045003 (2008).

[35] G. Gregori, A. Ravasio, A. Höll, S. H. Glenzer, and S. J. Rose, High Energ. Dens. Phys. **3**, 99 (2007).

[36] C. Lin (unpublished).

[37] G. Röpke, K. Kilimann, D. Kremp, W. D. Kraeft, and R. Zimmermann, Phys. Stat. Sol. (b) **88**, K59 (1978).

[38] R. Zimmermann, K. Kilimann, W. D. Kraeft, D. Kremp, and G. Röpke, Phys. Stat. Sol. (b) **90**, 175 (1978).

[39] For energy levels of atom and positive ions of carbon, see http://physics.nist.gov/PhysRefData/ASD/levels_form.html.

[40] L. B. Fletcher *et al.*, Phys. Rev. Lett. **112**, 145004 (2014).

[41] D. Kraus *et al.*, Phys. Rev. E **94**, 011202(R) (2016).

[42] A. Y. Potekhin, G. Massacrier, and G. Chabrier, Phys. Rev. E **72**, 046402 (2005).

[43] E. M. Apfelbaum, Phys. Plasmas **25**, 072703 (2018).

[44] B. B. L. Witte, L. B. Fletcher, E. Galtier, E. Gamboa, H. J. Lee, U. Zastrau, R. Redmer, S. H. Glenzer, and P. Sperling, Phys. Rev. Lett. **118**, 225001 (2017).

[45] M. Schöttler and R. Redmer, Phys. Rev. Lett. **120**, 115703 (2018).

[46] T. R. Preston *et al.*, High Energ. Dens. Phys. **9**, 258 (2013).

[47] M. Stransky, Phys. Plasmas **23**, 012708 (2016).

[48] A. Calisti, S. Ferri, and B. Talin, Contrib. Plasma Phys. **55**, 360 (2015).

[49] A. Calisti, S. Ferri, and B. Talin, J. Phys. B: At. Mol. Opt. Phys. **48**, 224003 (2015).

[50] D. R. Inglis and E. Teller, Astrophys. J. **90**, 439 (1939).

[51] C. Lin, G. Röpke, H. Reinholz, and W.-D. Kraeft, Contr. Plasma Phys. **57**, 518 (2017).

[52] M. Bethkenhagen (private communication).

[53] J.-F. Danel, L. Kazandjian, and R. Piron, Phys. Rev. E **98**, 043204 (2018).

[54] F. B. Rosmej, J. Phys. B: At. Mol. Opt. Phys. **51**, 09LT01 (2018)

[55] G. Röpke, J. Phys.: Conf. Series **569**, 012031 (2014).
[56] G. Röpke, T. Seifert, H. Stolz, and R. Zimmermann, Phys. Stat. Sol. (b) **100**, 215 (1980); G. Röpke, M. Schmidt, L. Münchow, and H. Schulz, Nucl. Phys. A **399**, 587 (1983); J. Dukelsky, G. Röpke, and P. Schuck, *ibid.* **628**, 17 (1998).
[57] D. Bollé, Ann. Phys. **121**, 131 (1979).
[58] M. D. Girardeau, Phys. Rev. A **41**, 6935 (1990).
[59] F. J. Rogers, Phys. Plasmas **7**, 51 (2000).
[60] W. Ebeling, W. D. Kraeft, and D. Kremp, *Theory of Bound States and Ionization Equilibrium in Plasmas and Solids* (Akademie-Verlag, Berlin, 1976).